

INTRODUCTION

Tetralogy of Fallot (TOF) is the most common cyanotic congenital heart disease (CHD) and represents about 5% to 7% of all CHD (*Lapierre et al., 2016*).

There is a broad spectrum of abnormalities, ranging from mild degree of obstruction of the RVOT up to severe degree with pulmonary atresia (*Lapierre et al., 2016*).

Classical TOF involves four typical features: ventricular septal defect, obstruction of right ventricular outflow tract, right ventricular hypertrophy and overriding of the aorta. Complex forms include TOF with absent pulmonary valve, TOF with pulmonary atresia with or without associated major aortopulmonary collateral arteries (MAPCAs) (*Banderker et al., 2015*).

In severe cases, pulmonary flow is maintained by a patent ductus arteriosus when the main pulmonary artery and its branches are intact and/or by major aortopulmonary collateral arteries (MAPCAs) when the pulmonary arteries are absent or severely hypoplastic. These MAPCAs are present since birth and are alternatives to the systemic pulmonary arterial flow (*Lapierre et al., 2016*).

The evaluation of this diverse anatomy is critical in the preoperative evaluation of a TOF patient to prevent on table surprises to the surgeon (*Khatrri and Shrivastava, 2010*).

The complex shape of the right ventricle renders it challenging for most of available imaging modalities. This is particularly true for the RVOT, which is essential for many congenital diseases, but has more complex anatomy and function (*Saremi et al., 2013*).

In different types of TOF, the anatomic heterogeneity, myriad of potential palliative surgeries and the possible associated intra cardiac and extra cardiac anomalies encountered must be taken into account when imaging patients with TOF (*Lluri et al., 2014*).

Echocardiography has become the standard imaging modality in the diagnosis of TOF (*Silverman, 2013*).

Echocardiography can be used for de novo diagnosis of this lesion, in determination of options for surgical interference (*Markley et al., 2016*).

Echocardiography is widely available, easy to perform, relatively cheap, with no hazard of ionizing radiation and provides proper anatomic and physiologic information about the right side of the heart; it still represents an adequate imaging modality for assessment of the right side of the heart (*Markley et al., 2016*).

However, as the RV is positioned close to the sternum and also being of complex geometrical shape, evaluation by 2D echocardiography may be limited (*Mustafa and Ashour, 2011*).

Moreover, it is limited in the assessment of certain portions of the aorta (particularly the ascending aorta and the arch), the RV, the distal pulmonary arteries, and the pulmonary veins (*Nakhla, 2015*).

Moreover, the diagnostic quality of echocardiography is highly dependent on the operator (*Stinn et al., 2011*).

Catheter angiography is an invasive approach with many disadvantages, like long sedation time, long procedure time, and arterial puncture complications. Cardiac magnetic resonance imaging (MRI) also has the same problems, as it necessitates long sedation time in the closed MRI. The spatial resolution of MRI is lower than that of CT, which can be a great drawback for visualizing small anatomical structures (*Soetikno and Hermawan, 2013*).

Multi detector CT affords excellent spatial resolution and rapid acquisition time and so, plays an expanding role in the assessment of cardiac and pulmonary structures in CHD patients (*Banderker et al., 2015*).

With the advancement of MDCT and increased experiences, the evaluation of intra cardiac anatomy has been further improved. The MDCT has several advantages like rapid data acquisition and large imaging field, which allow a complete delineation of the entire pulmonary vasculature and MAPCAs. At MDCT, all cardiac chambers and vessels can be

opacified with single injection of contrast medium. Also, MDCT offers high spatial resolution and cross-sectional images with 3D reconstruction (*Liu et al., 2016*).

MDCT frequently showed extra findings, like coronary anomalies, systemic or pulmonary venous abnormalities, pleural fluid collection, airway compression and pulmonary parenchymal disease, those were essential in the preoperative evaluation (*Liu et al., 2016*).

AIM OF THE WORK

The aim of this study is to assess the role of multi detector CT angiography in evaluation of right ventricle in patient with pulmonary atresia and Tetralogy of Fallot which plays an essential diagnostic value in determining appropriate patient management.

Chapter 1

RADIOLOGICAL ANATOMY OF RIGHT VENTRICLE IN PEDIATRICS

Background perception of cardiac anatomy is the first vital step to understand congenital heart disease. The major amount of the knowledge has been gained via surgical operations and correlation with the findings of catheter angiocardiology (*Goo, 2011*).

Considerable advances in MDCT scanners, software, hardware and post processing facilities have led to prompted improvement in displaying cardiac anatomy and pathology. The utilization of CT scanners with at least 64 detectors is currently standard and ECG-gating abilities are broadly accessible (*Terpenning and White, 2015*).

The heart includes three main portions: atria, ventricles and chief vessels (**Fig 1**). It should be known that each component having its precise morphologic characteristics rather than its spatial orientation in the body. A comprehensive studying of these characteristics is mandatory for the meticulous diagnosis of congenital cardiac diseases, particularly in complex forms (*Goo, 2011*).

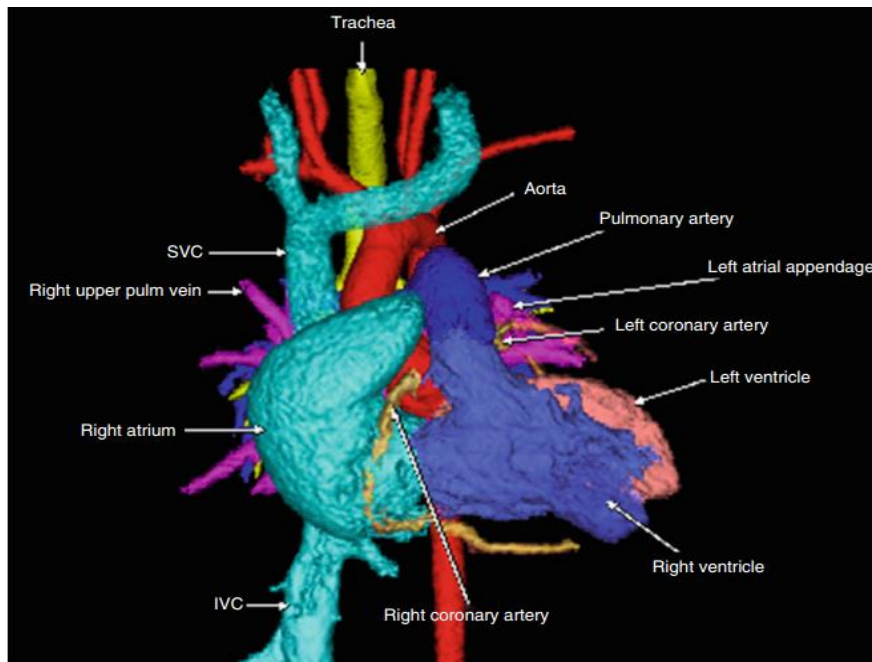


Fig. (1): Full color-coded 3D CT model reveals cardiac anatomy (*Quoted from Richardson, 2013*).

1. Cardiac Structures

Atria:

The atrium is a thin-walled chamber formed of the atrium proper and the atrial appendage. Both atria (**Fig 2**) are adjacent to each other on the ventricular base, the plane on which the valves situate and the inter-atrial septum separates them. The pectinate muscle is seen in the atrial appendage (**Fig 3**) and its extension is the most exact anatomic feature of atrial situs determination and situs of the thorax: situs solitus, situs inversus, and isomerism (*Goo, 2011*).

Considering 3D cardiac views from the top, the LA is seen at posterior aspect and on the left side yet the right one is seen at the anterior aspect and on the right (*Goo, 2011*).

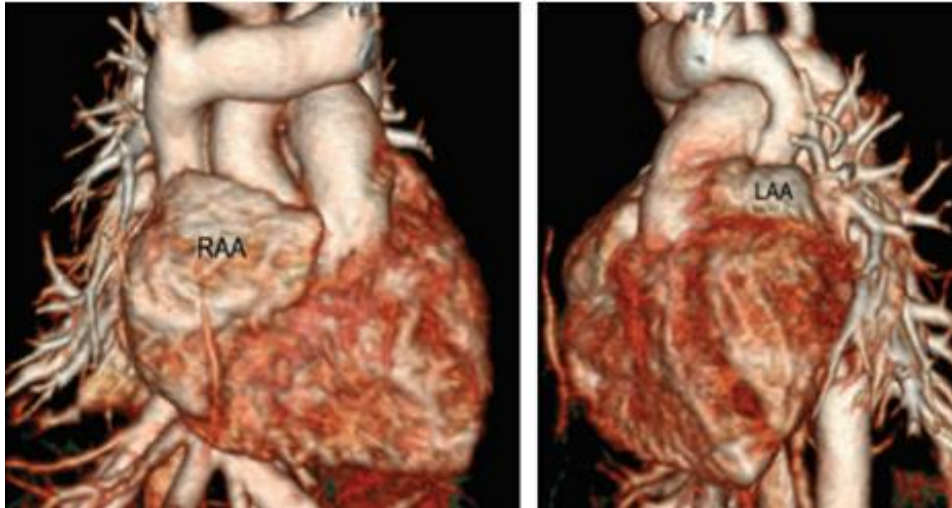


Fig. (2): 3D VR CT images show both atria with the right RAA characterized by its triangular appearance & the (LAA) (*Quoted from Goo, 2011*).

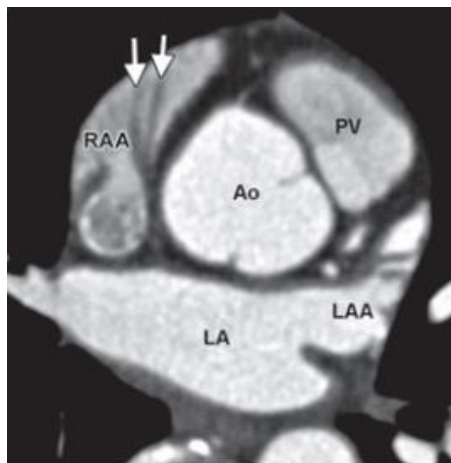


Fig. (3): CT axial view showing the right atrial appendage (RAA) has broader opening and prominent pectinate muscle (arrows) while the left one has a finger like shape (*Leschka et al., 2007*).

The Right Atrium

The right atrium is the cardiac chamber which receives systemic venous return via the superior and inferior vena cava (**Fig 4**) and coronary venous return via the coronary venous sinus (*Goo, 2011*).

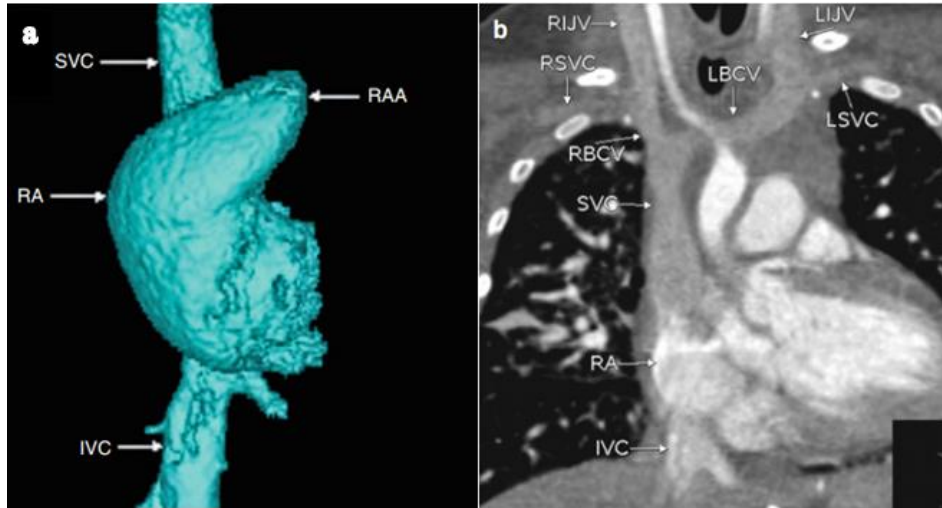


Fig. (4): 3D CT color coded anterior view (a) and CT coronal MIP view (b) image showing RA with RAA and systemic venous drainage (*Quoted from Richardson, 2013*).

Morphological appearance of the Right Atrium:

The right atrium is distinguished by its triangular broad appendage, also crista terminalis (**Fig 5**) which is a vertical ridge in between proper atrium and its appendage, also its connections with the coronary venous sinus and both vena cava (*Goo, 2011*).

The pectinate muscles of the atrial appendage reaches the nearby A-V connection so the atrium can be described as the morphological right one (*Goo, 2011*).

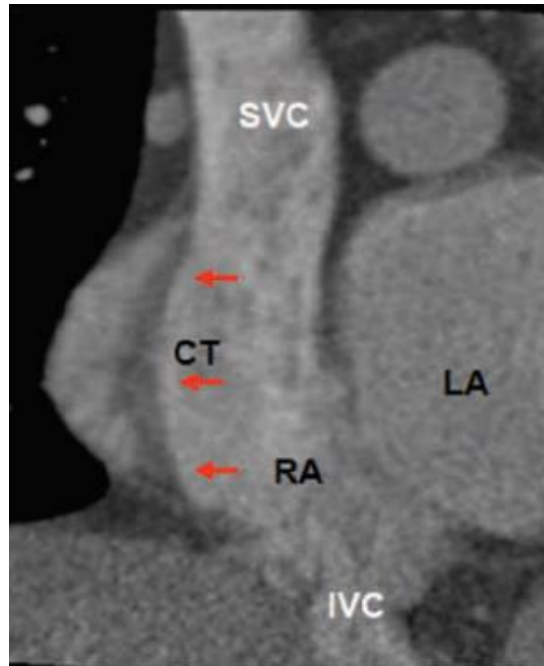


Fig. (5): CT Short axis view showing the crista terminalis, the characteristic of RA (arrows) (*Quoted from Saremi and Sanchez-Quintana, 2011*).

The Left Atrium (LA)

The left atrium is the most posterior cardiac chamber which receives pulmonary venous return via the four pulmonary veins (**Fig 6**) (*Goo, 2011*).

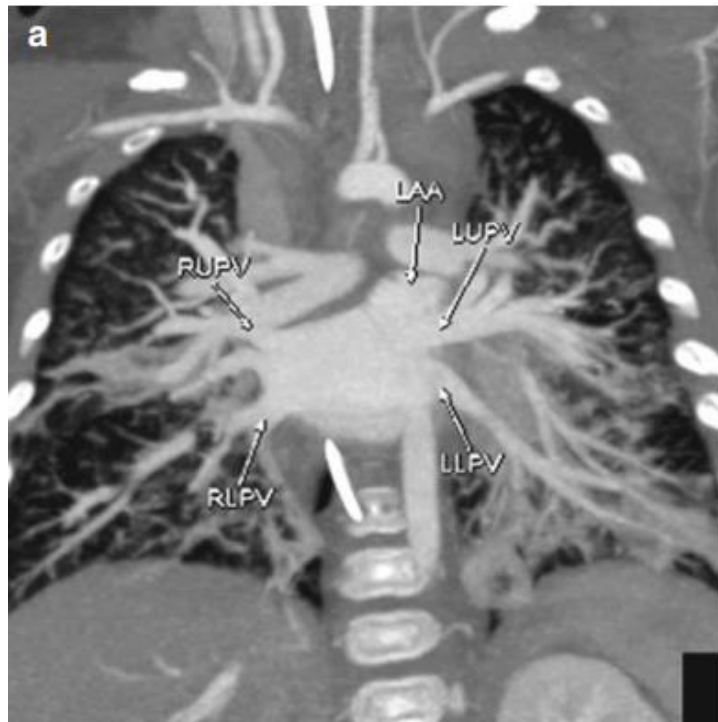


Fig. (6): CT Coronal MIP view showing superior and inferior pulmonary veins of both sides connected to the LA (*Quoted from Richardson, 2013*).

Morphological Features of the Left Atrium:

The left atrium is characterized by its narrow, hooked appendage, its connections with the four pulmonary veins, lack of the crista terminalis, with limited extension of the pectinate muscles of its appendage which don't extend to the nearby A-V junction (*Goo, 2011*).

The shape of the left atrium can be likened as an inverted box with its large opening committed to the mitral valve (*Goo, 2011*).

Ventricles

The ventricle is a muscular chamber that pumps blood to the great arteries. Similar to the atria, two ventricles are placed side by side at the ventricular base and inter ventricular septum separates them (**Fig 7**) (*Goo, 2011*).

The atrioventricular valve is nominated according to the ventricular morphology (e.g., the mitral valve for the morphological left ventricle, the tricuspid valve for the morphological right one) (*Goo, 2011*).

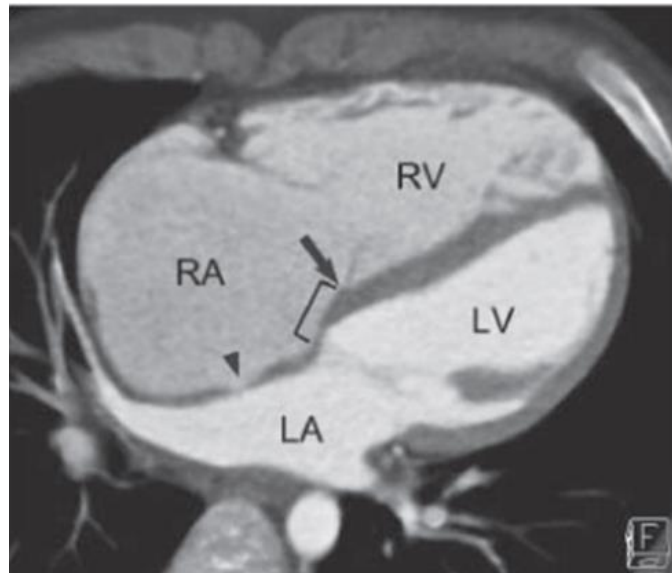


Fig. (7): 4-chamber cardiac CT view shows the four chambers and their relationships. The tricuspid valve (arrow) is slightly apical than mitral valve. The fossa ovalis is seen (arrowhead) (*Quoted from Goo, 2011*).

The Left Ventricle:

The left ventricle is a conical chamber having trabeculated walls which narrow down towards the rounded

cardiac apex. The boundaries, particularly between the posterior and septal walls, are indistinct. The LV opening is named ostium which gives attachment for the aortic annulus, the mitral valve and aortoventricular membrane (*Terpenning and White, 2015*).

The left ventricle is formed of inlet, outlet and apical portions and the inter-ventricular septum separates it from RV. This septum is classically seen bulging toward the RV due to the pressure difference (*Terpenning and White, 2015*).

The inlet is surrounded by the mitral valve and the outlet connects to the aortic valve. The anterior mitral valve cusp separates the outlet portion from the inlet. The outlet portion is incomplete posteriorly so that the cusps of the mitral and aortic valves are in fibrous continuity (**Fig 8**) (*Terpenning and White, 2015*).



Fig. (8): Double-oblique CT view showing LV inflow and outflow tracts, fine trabeculations and aortic-mitral fibrous continuity is noted (arrowhead) (*Leschka et al., 2007*).

The LV has two papillary muscles, the anterior and posterior muscles, (**Fig 9**) that are larger than those of the RV. The chordae tendinae are seen attaching the papillary muscles to the cusps of mitral valve (*Terpenning and White, 2015*).

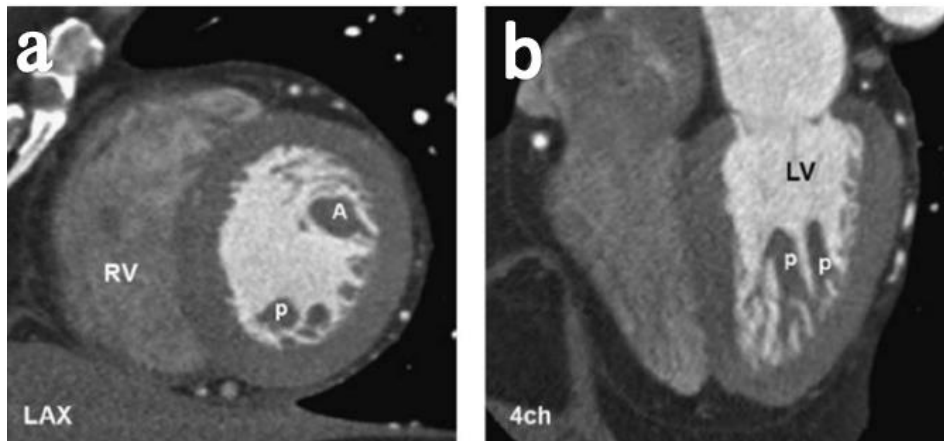


Fig. (9): a) Short-axis and b) four-chamber CT views displays the anterior (A) and posterior (P) papillary muscles. The anterior one is larger and less tethered to the LV wall (*Quoted from Saremi and Sanchez-Quintana, 2011*).

The LV apical trabeculated part is seen extending to the apex. It is specified by its fine trabeculations, (**Fig 10**) in comparison to those of the RV, which is a useful feature in the diagnosis of ventricular morphology in congenital diseases (*Terpenning and White, 2015*).



Fig. (10): Vertical long-axis CT image of the LV reveals trabeculations, papillary muscles, and tendinous cords attached to the mitral valve. Two layered myocardium, outer compacted and inner non compacted (arrows) (*Quoted from Goo, 2011*).

Right ventricle:

The RV is the most anterior cardiac chamber just behind the sternum which is bordered by the annulus of the pulmonary and tricuspid valves (*Markley et al., 2016*).

RV is specified by its complex shape and structure. It looks crescent-shape when viewed in cross-section and triangular when viewed from the side view, in contrast to the left ventricle which looks ellipsoidal in shape. The position of inter ventricular septum might affect the RV shape. Under normal situations, the septum is seen concave toward the left ventricle in the systole and diastole (*Sadeghpour and Alizadehasl et al., 2015*).